A Tracking Cooling Fan Using Geofence and Camera-Based Indoor Localization

LIU Shuo [a,*], YIN Le [b], HO Weng Khuen [a], LING Keck Voon [b], SCHIAVON Stefano [c]

[a] *Department of Electrical and Computer Engineering, National University of Singapore, Singapore 119077*

[b] *School of Electrical and Electronic Engineering, Nanyang Technological University, Singapore 639798*

[c] *Center for the Built Environment, University of California, Berkeley, CA 94720, USA*

*Corresponding author. Tel.: +65-97156453
E-mail address: s_liu01@u.nus.edu

Highlights

- Human positions are tracked accurately by a camera-based indoor tracking system
- Air flow is directed to the desired direction by using virtual geofences
- Desired air speed is provided based on the PMV-SET thermal comfort model
- Fan speed setting is adjusted by a calibrated mapping algorithm based on the estimation of occupant-fan distance
- The proposed system can be used for thermal comfort improvement and energy conservation

Abstract

Compressor-based cooling systems have a large impact on energy consumption in modern buildings, particularly in the tropics. Elevated air movement by electric fans is a cost-effective cooling method for both energy saving and thermal comfort improvement. In this paper, a tracking cooling fan using geofence and camera-based indoor localization is proposed. Personal cooling service is provided based on the detection of the occupant in the area bounded by virtual geofences. The proposed camera-based indoor tracking system is able to accurately locate the positions of the occupant, determine the direction of air flow, and calculate the occupant-fan distance. The tracking fan is able to provide the needed air speed determined by PMV-SET thermal comfort model using a calibrated mapping algorithm. The effectiveness of the proposed system has been verified through experiments which show that the system is able to operate with low power while improving thermal comfort. The system can be used in an air-conditioned environment with higher temperature setpoint to save energy or in a naturally conditioned environment for thermal comfort enhancement.

Keywords

Tracking cooling fan; Geofence; Indoor localization; Thermal comfort; Energy savings; Air movement

1. Introduction

In warm climates, compressor-based cooling is the main contributor to the energy consumption in buildings. In the United States, compressor-based cooling accounts 13% and 14% of primary energy consumption in commercial and residential buildings respectively (DOE 2011). In tropics such as Singapore, the electricity consumed by air conditioning comprises up to 50% of total electricity usage by buildings (NEA 2010). Timing and quantity of energy use associated with cooling have large impacts on cost, greenhouse gas emission, peak load of electricity use and reliability of electrical grid.

Raising cooling setpoint of air conditioning system can both bring financial benefits (Sekhar, 1995; Schiavon & Melikov 2008; Hoyt et al. 2015; Rim et al. 2015; Duarte et al. 2016) and reduce negative impact on the environment (NCCS & NRF 2011) but it may run the risk of sacrificing the comfort level felt by occupants, directly influencing their health, well-being, and productivity.

The challenge can be overcome through elevated air speed generated by electric fans which is a cost-effective and energy-efficient cooling method. Unlike compressor-based cooling systems which lower the air temperature and humidity, electric fans increase the air movement around people. Air movement has significant cooling effect and increases the acceptable range of indoor temperatures (Mcintyre 1978, Zhai et al. 2013, Schiavon et al. 2016). It can be used in conjunction with the air conditioning system.

Figure 1: An example of how occupant position may change in time.

Most of cooling fans are not connected to the building management system (BMS) and the few that are connected operate based on maximum occupancy assumption, fixed air speed and schedules. Buildings lack intelligent reasoning to customize the fan operation to meet the needs

of occupants resulting in wasted energy and sub-optimal thermal comfort. This could be due to the following points:

(a) Fans do not know the positions of people. This may cause inconvenience in the cases that the occupant is not willing or does not have the chance to redirect the fan or manually adjust the fan speed, especially when an occupant moves along his workspace or in the building (Figure 1). Hence both the direction at which the fan blows air and the fan speed setting should be changed accordingly.
(b) There is lack of real-time input of occupancy information to the BMS, such as the number and positions of occupants. It is difficult to track the positions of an occupant in a dynamic indoor environment where the layout and the occupancy keep changing.
(c) Traditionally, air speed is not measured due to the high cost of omnidirectional hot-wire anemometers.

For the points mentioned above, (a) and (b) refer to the issue of occupancy detection and tracking for fans operation. Point (c) is about the air speed measurement for thermal comfort. The aim of this paper is to develop a tracking cooling fan system to address the problems stated above.

1.1 Occupancy information for cooling

Occupancy information plays an important role in building cooling and fan operation. For the heating, ventilation and air condition (HVAC) system, Daikin employs "intelligent eye" infrared sensor (Daikin, online material) to detect human movement but it is no more than ascertaining whether or not there are people in the room. Mitsubishi utilizes eight "move-eye" infrared sensors (Mitsubishi, online material) in their air conditioning system for human and environment detection by acquiring thermographic data. However, using the infrared sensor may not be accurate on measuring the skin temperature if the sensor is far from the person. Additionally, it is household-oriented and may not be suitable for personal cooling in the office environment. Previously developed smart fans (Xia et al. 2010, Zhou et al. 2014) are able to direct the air towards people based on the occupant detection but adjustment of fan speed is not considered. Other smart systems (Liu 2013, Arens et al. 2015) determine the fan speed setting by temperature or humidity but the occupant-fan distance is neglected. Since the air speed attenuates during the propagation, the distance has great influence on the thermal sensation on people.

A number of developed human detection and tracking solutions can be found in the literature, including PIR (passive infrared) sensor (Dodier et al. 2006, Duarte et al. 2013, Kim et al. 2013), RFID (radio-frequency identification) (Ni et al. 2004, Zhou & Shi 2011, Li et al. 2012) and CO_2 sensor (Sun et al. 2011, Shan et al. 2012). While each of these methods has advantages, it also has its own limitations. For example, PIR sensors based approaches are compromised by other heat sources with strong radiation (e.g., the direct or reflected sun radiation) and can only provide binary information indicating the presence/absence of a person (Li et al. 2012). Most RFID-based systems rely on proximity detection of mobile readers by tags which could be expensive and the density of reference tags is crucial and hard to determine (Rana et al. 2015). The performance of CO_2-related solutions highly depends on the calibration and commissioning of measurement instrumentations (Sun et al. 2011).

Custom-digitized geofence has emerged as a significant area of interest for location-based service (LBS) over the last decade. A geofence is defined as a virtual perimeter for a real-world geographic area and LBS can be delivered when a target enters or exits a geofence. Reclus & Drouard (2009) presents fundamental concepts of geofencing and its applications in the transport and logistics sector. Munson & Gupta (2002) discusses geofence-based notification as general-purpose service from commercial promotion to tourism, traffic information, public service and safety. Namiot & Sneps-Sneppe (2013) employs network proximity rules as geo-based boundaries to effectively deploy indoor location based services and provide significant energy saving for mobile devices compared with the traditional methods.

In this paper, a tracking cooling fan using geofence and camera-based indoor localization is proposed for thermal comfort and energy savings. The cooling area of the electric fan is divided into several sub-area bounded by predefined geofences. By detecting the occupant enter which geofenced sub-area, the direction of air flow is determined. Compared to infrared radiation based PIR sensor or proximity detection based RFID, camera-based vision analysis technique (Benezeth et al. 2011, Jia & Radke 2014, Gaspar & Oliveira 2015) for indoor tracking is able to provide highly accurate position estimates with the resolution being from 0.01 cm to 1 cm (Mautz 2012). The approach brings convenience for the occupants since there is no need for them to carry extra devices. The proposed indoor tracking system identifies the tracked targets from the images taken by the camera fixed in the tracking area and the captured images are then checked against a pre-calibrated database to give position estimates. The system estimates the position of the occupant, determines the direction of air flow, and calculates the occupant-fan distance. The input power of the geofenced fan is then automatically adjusted by a calibrated mapping algorithm to generate the desired air speed.

1.2 Air speed for thermal comfort

The potential of comfort improvement and energy saving by elevated air speed is often ignored due to the strict limits set by thermal comfort standards such as ASHRAE 55-1992/2004 and Singapore Standard SS 553:2009 (SSC 2009). Additionally, the most commonly used thermal comfort assessment tool, the PMV (Predicted Mean Vote) index, is not sufficiently accurate in elevated air movement conditions (Arens et al. 2009). However, recent studies of occupied buildings provide consistent evidence that large percentages of occupants prefer more air movement than what they currently have in conditions perceived as warm, thermally neutral and even slightly cool (Arens et al. 2009). According to the latest ASHRAE Standard 55-2013 (ANSI/ASHRAE 2013), air speed could have no limits or up to 0.8 m/s depending on whether or not the occupant control of air speed is available. In the proposed system, the electric fan is pre-calibrated to obtain the relationship between air speed and fan input power by measuring air speed at different target-fan distances before real-time implementation. The effect of elevated air speed on the sensation of thermal comfort can be assessed through the PMV-SET (Predicted Mean Vote – Standard Effective Temperature) thermal comfort model. In this paper, the PMV-SET model is also used to determine the desired air speed.

2. Methods

2.1 Tracking cooling fan system architecture

The flow chart of the proposed system is shown in Figure 2. The system engine first estimates the position of the occupant and the fan will be automatically switched on/off depending on whether or not the occupant enters the cooling area bounded by predefined geofences. Based on the estimated position $(\hat{x}, \hat{y})$, the system engine then calculates the slope of the straight line crossing $(\hat{x}, \hat{y})$ and the position of the fan located at the original point $(0,0)$ to direct air flow, and also the occupant-fan distance for fan power determination.

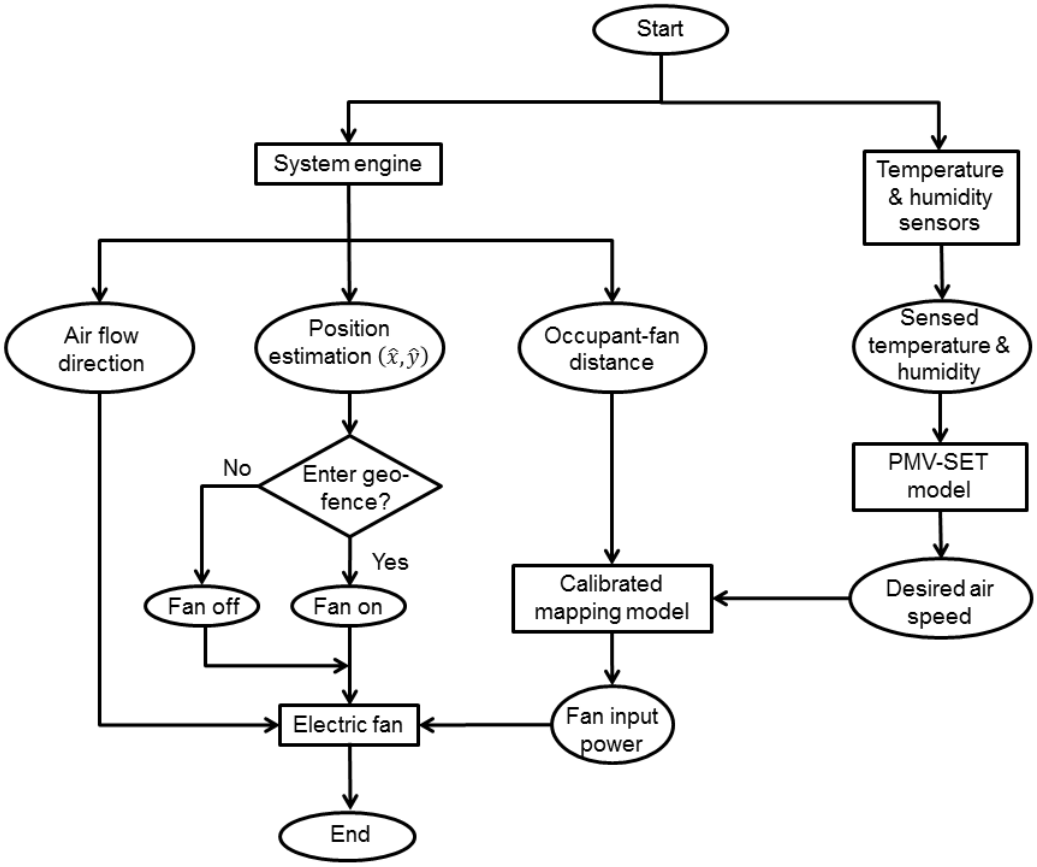

Figure 2: Flow chart of the proposed system.

A calibrated mapping algorithm is proposed to find suitable fan input power to generate elevated air movement, meeting the thermal comfort requirements. In addition to the occupant-fan distance, another input to the calibrated mapping algorithm is the desired air speed determined by the PMV-SET model. There are six primary variables affecting PMV value, including four environmental variables: dry-bulb air temperature, mean radiant temperature, relative humidity, air speed and two personal variables: metabolic rate and clothing insulation. In a real-time implementation, room temperature and relative humidity are sensed to access the human sensation via the PMV-SET model while all the other parameters are predetermined. If cost-effective sensors become available these can easily be incorporated in the existing architecture. The desired air speed is then calculated by setting suitable PMV values in the comfort zone.

2.2 Experimental facilities and instruments

The experiments have been conducted in a large open-space office environment. A typical cubic-desk workstation shown in Figure 1 was chosen as the area tracked by the camera where the dry-bulb temperature and the mean radiant temperature could be assumed to be the same since there are no significant radiant sources and the workstation is far from windows.

The system employs a three-phase brushless direct current (DC) fan (Model FSAW98RI-A, Airmate, China) which provides 32-level speed settings. The noise varies from 29 dB to 59 dB depending on the selected setting level. The fan power ranges from 3.8 W to 19.3 W when the speed setting is set from level 1 to level 20 (Table A1 in the Supplementary Information). The fan power was measured using a power meter (Energy monitoring socket, Efergy, UK) with the accuracy of $\pm$2% of readings.

The images used in the experiments for vision analysis were taken by a normal cell phone camera (Model Exmor RS, Sony) of which the frame rate can be as high as 30 frames per second and the attached IMX135 CMOS sensor provides the maximum resolution of 4224 × 3176 pixels.

During the evaluation phase, but not for the operation phase, the air speed was measured using a hot-wire anemometer (AirDistSys5000, Sensor Electronics, Poland). The omnidirectional, spherical speed sensor has a diameter of 2 mm and provides measurement range of air speed from 0.05 m/s to 5 m/s with the accuracy of ±0.02 m/s ±1.5% of readings.

2.3 Experimental conditions

Since the air conditioning system is usually set around 23°C in tropical climates (Sekhar 2016, Sekhar 1995), it is proposed to increase the setpoint to save energy. Assuming that the dry-bulb air temperature (t_a) is the same as the mean radiant temperature ($\overline{t_r}$), we consider three operative temperature (t_o) categories: 26°C, 27.5°C and 29°C (79°F, 82°F and 84°F). Based on the work of Schiavon et al. (2016), it is expected that in tropical climate for office work conditions, 29°C is the upper acceptable limit.

Five occupied positions shown as circles in Figure 4(a) were selected for testing. For each temperature category, the air speed was measured at each test position based on the fan input power calculated by the proposed method. The mean values of measured data were then compared with the theoretical desired air speeds based on the PMV-SET model for evaluating the performance of the proposed system.

2.4 Localization algorithms and geofencing

The proposed indoor tracking system utilizes vision analysis to estimate positions of the occupant. An illustration on how the system localizes a target is shown in Figure 3. A reference marker as the target to be tracked was placed behind the chair as shown in Figure 3(a). By tracking the representative pixels referring to the reference marker, the position of the occupant can be estimated as shown in Figure 3(b) based on a pre-calibrated database which contains the mapping information from indexes of pixels in the image to physical dimensions of the tracking area. The camera was placed in the ceiling with an angle of depression to take the tracking area into the field as shown in Figure 4(b).

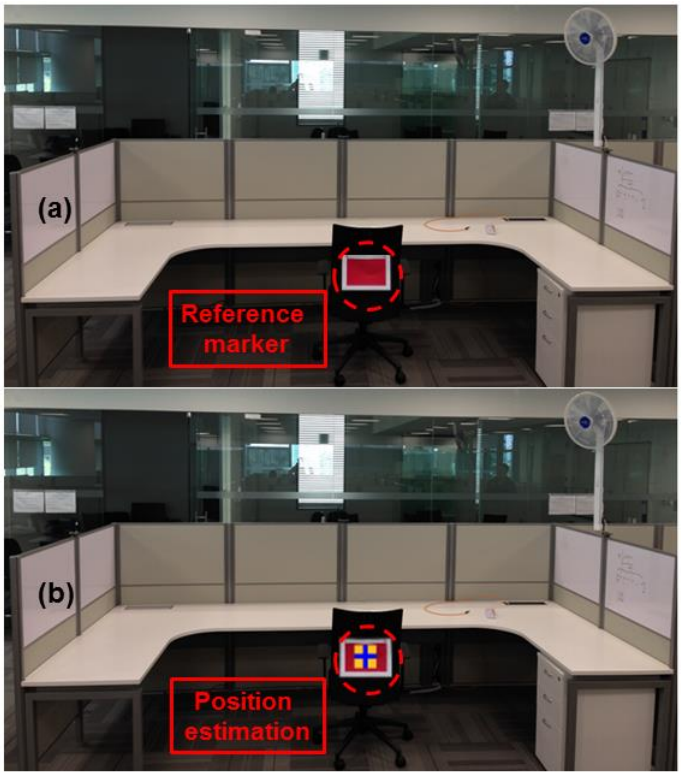

Figure 3: Illustration of localizing a target: (a) identification of a reference marker; (b) position estimation.

The size of the cooling area by the fan depends on the fan coverage area and the expected area of occupancy and can be customized for real furniture layout. These two metrics can be same or different and in this case we selected an example in which expected occupancy area is smaller than fan coverage area. Since the size of the used cubic desk shown in Figure 3 is 3.7 m × 2.0 m and the maximum fan-occupant distance is $\sqrt{3.7^2 + 2.0^2} = 4.2$ m, the cooling area of the fan is therefore defined as a quarter circle with the center *O* and the radius of 4.5 m (> 4.2 m) as shown in Figure 4(a). The judgment condition of entering the cooling area is defined as $\{0 < \hat{x} < 3.7$ m, $0 < \hat{y} < 2.0$ m$\}$. If no one is detected in a preset time interval, the fan will be automatically switched off.

The fan is designed to be placed at the original point *O* (0,0), beside the workstation. The fan can oscillate from 0° to 90° in the coordinate system as shown in Figure 4(a) and the circular sector of the cooling area is divided into three equal sub-area Ⅰ, Ⅱ, Ⅲ of each with an angle of 30°. Each sub-area is bounded by predefined geofences. A geofence is defined here as a virtual perimeter to form a sub-area where the occupant is localized and is used for the determination of the air flow direction. For example, if an occupant is localized in sub-area Ⅰ, the fan will then be redirected to blow air at sub-area Ⅰ. By calculating the slope $k = \hat{y}/\hat{x}$ of the straight line which crosses the points $(\hat{x}, \hat{y})$ (the estimated position) and *O* (0,0) (the location of the fan), two straight geofences with slopes k = 0.58 and k =1.73 respectively in the coordinate system, were selected as the boundaries to separate the three sub-area. The direction of air flow is then a

function of k: if $0 < k \leq 0.58$, air flow is directed to sub-area Ⅰ; if $0.58 < k \leq 1.73$, then the fan blows air at sub-area Ⅱ; else sub-area Ⅲ is selected.

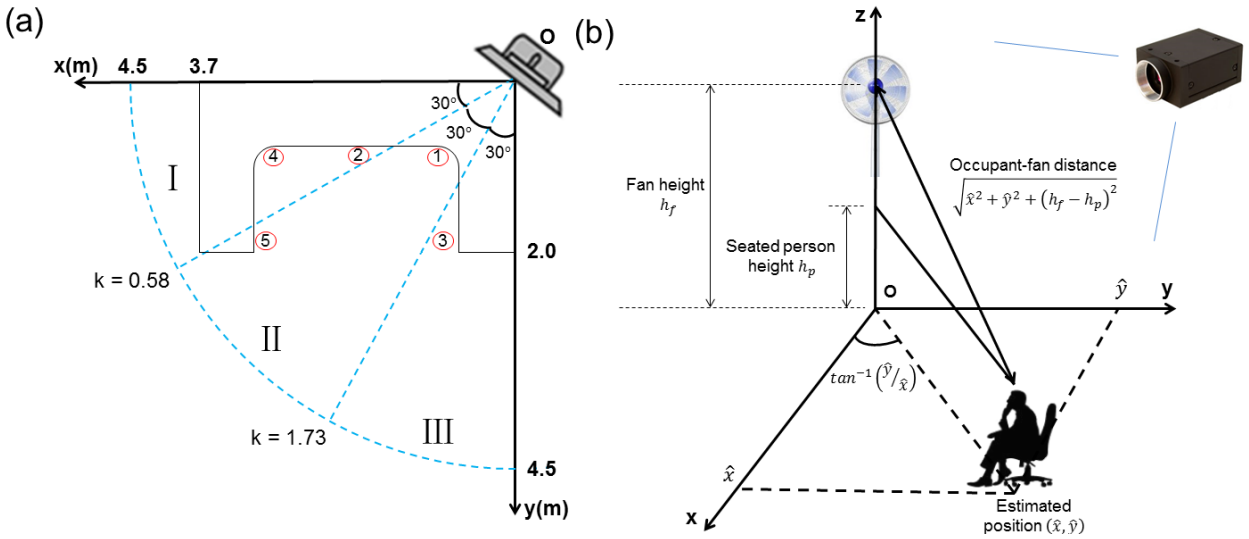

Figure 4: Localization algorithms: (a) direction of air flow determination (dashed curves: predefined geofences; stars: test positions); (b) occupant-fan distance calculation.

The fan is placed with an arbitrary height, h_f, known to the system (i.e. at h_f = 2.3 m in Figure 4(b)). In warm environments, the head region is one of the dominant body parts affecting overall comfort (Zhang & Zhao 2007, Zhang et al. 2010a, Zhang et al. 2010b, Zhang et al. 2010c) and the head height of a seated person, h_p, is assumed to be 1.1 m according to thermal comfort standards. The occupant-fan distance is therefore calculated as $\sqrt{\hat{x}^2+\hat{y}^2+(h_f-h_p)^2}$ as shown in Figure 4(b), which will be used for fan power determination. The height can be changed and adapted to different conditions.

2.5 Thermal comfort assessment: PMV-SET model

The PMV-SET model or the elevated air speed model (ANSI/ASHRAE 2013, Schiavon et al. 2014) is a two-step procedure comprising first using the PMV model to determine the comfort zone at the still-air region ($V \leq 0.2$ m/s) and then utilizing the SET index to extend the comfort zone to the elevated-air-speed region ($V > 0.2$ m/s). The idea was first described in (Arens et al. 2009) and then an issue was found by Yang et al. (2015). An updated model has been proposed and the latest ASHRAE standard 55-2013 adopts this change. The core structure of the PMV-SET model is described below.

Consider functions, *PMV* and *SET*, with the six parameters. Let t_a be the average air temperature, $\bar{t_r}$ be the mean radiant temperature, V_{elev} be the elevated average air speed and the average speed in still air, $V_{still} = 0.2$ m/s. The cooling effect, *CE*, due to the elevated air speed could be obtained by iteratively solving the following equation:

$$SET(t_a, \bar{t_r}, V_{elev}, *) = SET(t_a - CE, \bar{t_r} - CE, V_{still}, *) \quad (1)$$

where * denotes the invariant parameters which should be the same for both cases. Eq.(1) means that the adjusted average air temperature, $(t_a - CE)$, and adjusted mean radiant temperature, $(\bar{t_r} - CE)$, at still air yields the same SET value as the actual average air temperature and actual mean radiant temperature do at elevated air speed. Eq.(1) can be solved by using the secant and bisection iterative algorithm. Once the *CE* is obtained, then the adjusted PMV value in the still-air zone is given by

$$PMV_{adj} = PMV(t_a - CE, \bar{t_r} - CE, V_{still}, *) \quad (2)$$

The desired air speed is determined by the PMV-SET model and the model parameters are summarized in Table 1. All the target air speeds under different temperatures are limited to 0.8 m/s without occupant control, according to ASHRAE standard 55 (ANSI/ASHRAE 2013). This constraint can be removed in case the standard changes in future.

Table 1: PMV-SET model parameters (*RH* = 50%, *M* = 1.2 met).

Operative temperature t_o (°C)	Clothing insulation	Target PMV	Desired air speed V_d (m/s)
26	0.7	0.00	0.55
27.5	0.6	0.15	0.64
29	0.5	0.30	0.78

In this example, as shown in Table 1, relative humidity, *RH*, was assumed to be 50%. Metabolic rate, *M*, was set to be 1.2 met for typical office work. We assumed that the warmer the temperature was, the less clothing people would put on. The typical value of business clothing in the tropics is 0.7 clo (short sleeve button or polo shirt, long trousers, socks, business shoes and office chair). With higher cooling setpoints the clothing insulation was reduced down to 0.5 clo (recommended value for summer conditions), expecting people to dress according to the indoor climate. This assumption can be changed freely.

For the purpose of keeping occupants comfortable in a warm environment, the target values of PMV are limited to the range from 0 to 0.5. For lower temperatures, the PMV value at each position can be set as zero, representing thermal neutrality. However, for higher temperatures, we used slightly higher PMV values. We did this with the objectives to minimize the air flow intrusion to other desks and to avoid violating the limit of air speed being 0.8 m/s according to thermal comfort standard.

2.6 Calibrated mapping algorithm

In this section, a calibrated mapping algorithm is proposed to find suitable fan input power to generate desired air speed. The rationale is that the air speed can be regarded as a natural logarithm model of fan power (Yang et al. 2015). Thus the model parameters need to be identified.

The measuring point of air speed was placed at different distances away from the fan from 0.5 m to 4.5 m in step of 0.5 m. At each distance, 20 measurements, each corresponding to a specific fan input power, were taken. The air speeds were measured at 1.1 m height which is the same as the height of fan blade center. At a sampling interval of 2 s, each measurement took 90 samples

over 3 min. In total 90 × 20 × 9 = 16200 samples were measured. Then the average values (Table A1 in the Supplementary Information) were used to fit the curves between air speed and fan power using the least-squares criteria.

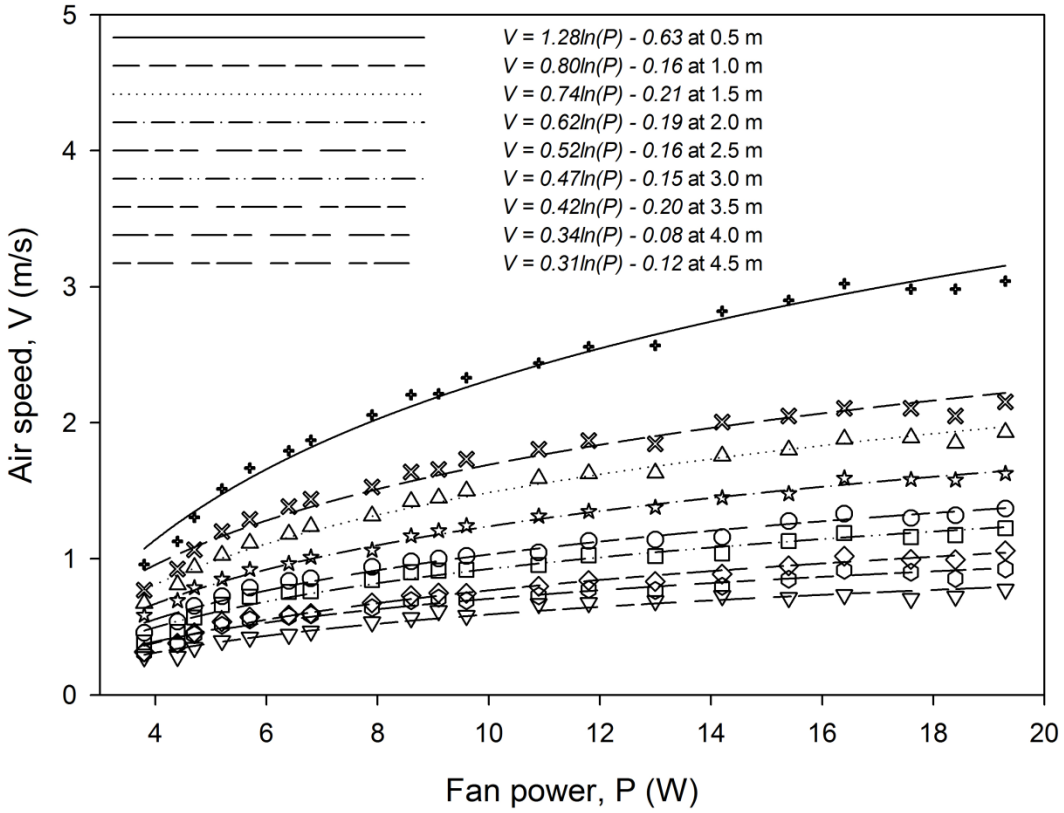

Figure 5: Natural logarithm model between air speed and fan power (average air speeds are given by the symbols).

The fitted natural logarithm curves at different distances are shown in Figure 5 where the average air speeds are shown as scatter plots. It can be seen that the average values of the measurements fit the curves well. The mean absolute error, e_{ma}, and the root mean square error, e_{rms}, between the measured air speeds and the fitted curves are summarized in Table 2. The former metric shows the absolute deviation of measured data from fitted curves while the latter amplifies and severely punishes large errors.

As shown in Table 2, both e_{ma} and e_{rms} at all distances are less than 0.07 m/s which is good enough for our purpose. In real-time application, the calculated occupant-fan distance will be compared to the 9 calibrated mapping curves at different distance from 0.5 to 4.5 m as shown in Figure 5, and the curve with the nearest deviation to the calculated distance will be selected to determine the fan input power.

Table 2: Errors between measured air speeds and fitted curves in fan power.

Distance (m)	Natural logarithm curves	
	e_{ma} (m/s)	e_{rms} (m/s)
0.5	0.07	0.07
1.0	0.06	0.07
1.5	0.04	0.04
2.0	0.02	0.03
2.5	0.03	0.04
3.0	0.03	0.04
3.5	0.02	0.03
4.0	0.03	0.03
4.5	0.02	0.03

3. Results and analysis

3.1 Localization results

The localization results are summarized in Table 3. As shown in Table 3, the estimated coordinates of the five tested positions are given in the 2nd column. Once this information is available, the slope of the straight line crossing the original point and estimated position, and the occupant-fan distance can be calculated as shown in the 3rd and the 5th columns respectively. The former metric is used to decide at which sub-area the fan should blow air while the latter one helps to select the most suitable calibrated mapping curve for fan power determination.

Table 3: Localization results of the five test positions.

Test positions	Estimated position $(\hat{x}, \hat{y})$	Slope k = $\hat{y}/\hat{x}$,	Air flow direction	Occupant-fan distance (m)	Calibrated mapping curve
1	(0.8,0.9)	1.13	II	1.7	1.5 m
2	(1.7,0.8)	0.47	I	2.2	2.0 m
3	(0.8,1.9)	2.38	III	2.4	2.5 m
4	(2.8,0.9)	0.32	I	3.2	3.0 m
5	(2.8,1.9)	0.68	II	3.6	3.5 m

3.2 Fan power determination

Based on the PMV-SET model, the target air speeds for 26°C, 27.5°C and 29°C cases are determined as 0.55 m/s, 0.64 m/s and 0.78 m/s respectively. Note that the target air speeds at different positions under the same temperature are the same due to the fair assumption that the room temperature is uniform in the area of the cubic desk.

By considering the effect of occupant-fan distance on the air speed felt by the occupant, the fan power at different positions is determined as different values. This is done by selecting different mapping curves, each labeled by a unique distance. Based on the estimated positions, the

calibrated mapping curves used to calculate fan power at test positions under different temperatures are shown in Figure 6.

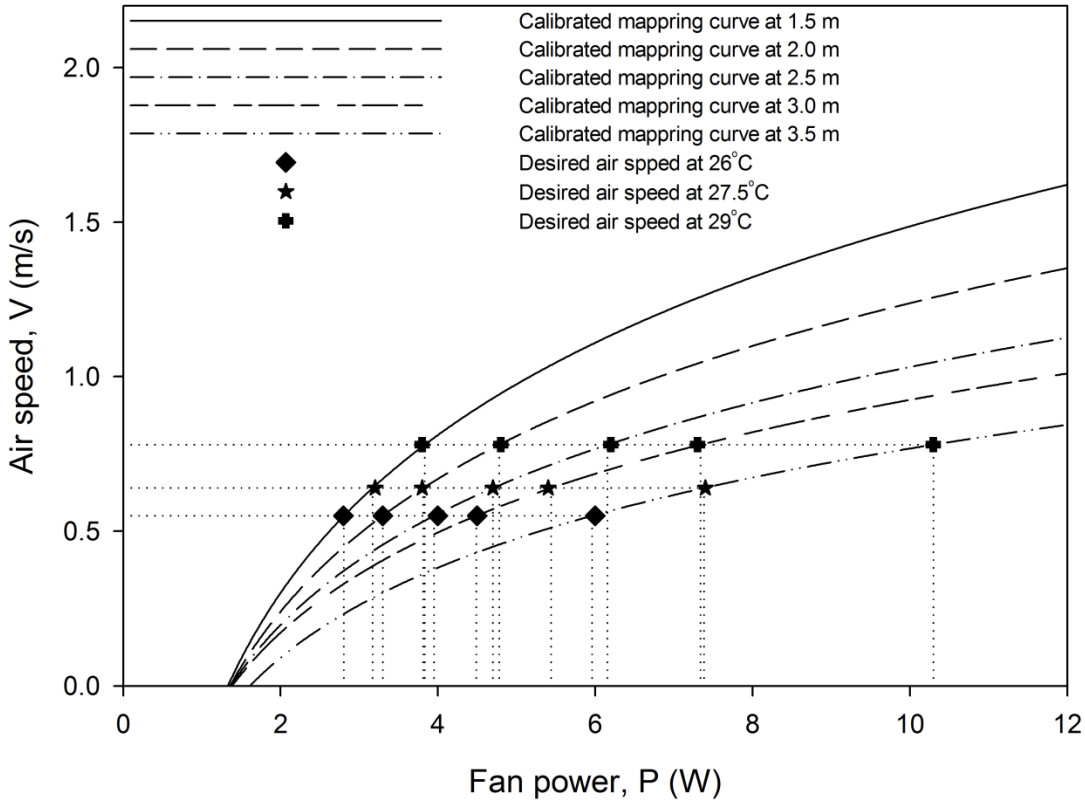

Figure 6: Fan power determination by the calibrated mapping algorithm.

The obtained results of fan power are explicitly summarized in Table 4. In Table 4, we can see that the fan power in all tested conditions is low, less than 11 W. The obtained fan input power was then applied to the electric fan and the corresponding air speed at each test position was measured for different temperature categories.

Table 4: Obtained fan power at target positions.

Test positions	Fan input power (W)		
	26°C category: target air speed 0.55 m/s	27.5°C category: target air speed 0.64 m/s	29°C category: target air speed 0.78 m/s
1	2.8	3.2	3.8
2	3.3	3.8	4.8
3	4.0	4.7	6.2
4	4.5	5.4	7.3
5	6.0	7.4	10.3

3.3 Air speed measurement

To verify the effectiveness of the proposed method, we employed the fan power obtained at Position 1 as the baseline data and measured the resulting air speed at the other positions without modifying the power input. This would be the situation before the implementation of the algorithm proposed in this paper. The resulting measured air speeds are shown as box-and-whisker plots in Figure 7(a). As a comparison, the measured results by using the proposed method were plotted in Figure 7(b). The graphs are developed using SigmaPlot 10.0 and each plot contains 90 measured samples taken at one position for 3 min using a 2-s sampling rate.

In Figure 7, with the position changing from 1 to 5, the occupant-fan distance increases. It can be seen that the variance of the air speed measurements increases with distance due to the typical behavior of isothermal jets. Nevertheless, the standard deviation is less than 0.1 m/s. The details of air speed measurements in Figure 7 are given in Supplementary Information (Table A2).

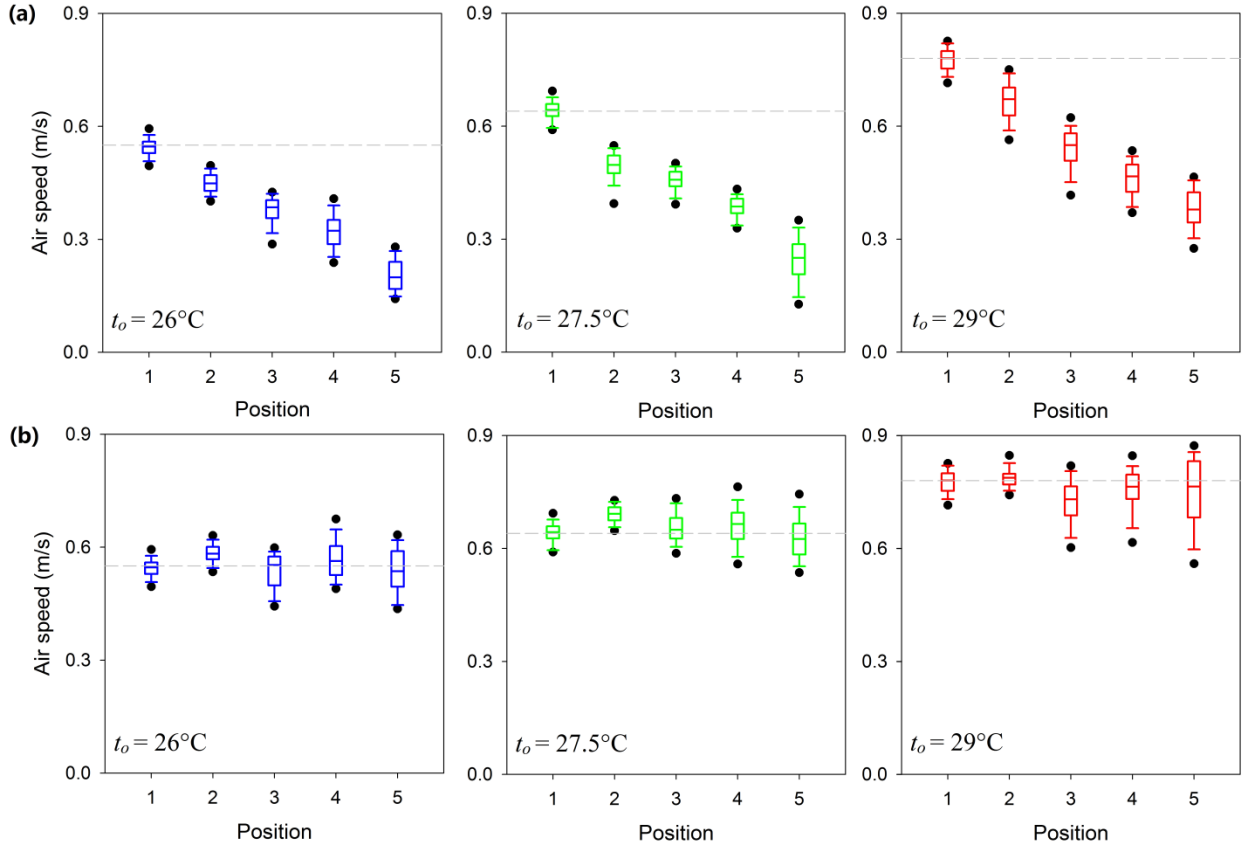

Figure 7: Air speed measurements: (a) without proposed method; (b) with proposed method. The target air speeds, 0.55 m/s, 0.64 m/s and 0.78 m/s for 26°C, 27.5°C, and 29°C respectively, are shown as dashed lines.

As shown in Figure 7(a), the air speeds deviate away from the targets when the distance increases. Without the mapping algorithm, it is difficult to find a suitable fan power to meet the requirement of thermal comfort. Though a specific fan power is applicable at one position, it may not satisfy the occupant when he or she moves to other positions. On the contrary, in Figure 7(b), using the proposed calibrated mapping algorithm is able to maintain the air speeds around

the target values for all temperature categories since the air speed generated by the fan is customized for different occupant-fan distances. With suitable fan power provided, the fan is able to generate the desired air speed and wasted energy is avoided.

3.4 Thermal sensation with elevated air speed

The effect of elevated air speed on thermal sensation is assessed using the PMV-SET model. The target PMV values for 26°C, 27.5°C and 29°C cases are 0.00, 0.15 and 0.30 respectively. The PMV values corresponding to the air speed measurements (in Figure 7) are plotted in Figure 8 and the statistical analysis is given in Supplementary Information (Table A3). For the case without the proposed method, the PMV values deviate from the targets with increased distance and even go outside the thermal comfort range at farther positions. With the proposed calibrated mapping algorithm, PMV at each test position varies around the target value. For all the three temperature categories, the corresponding thermal sensation is within the comfort zone (-0.5 < PMV < 0.5).

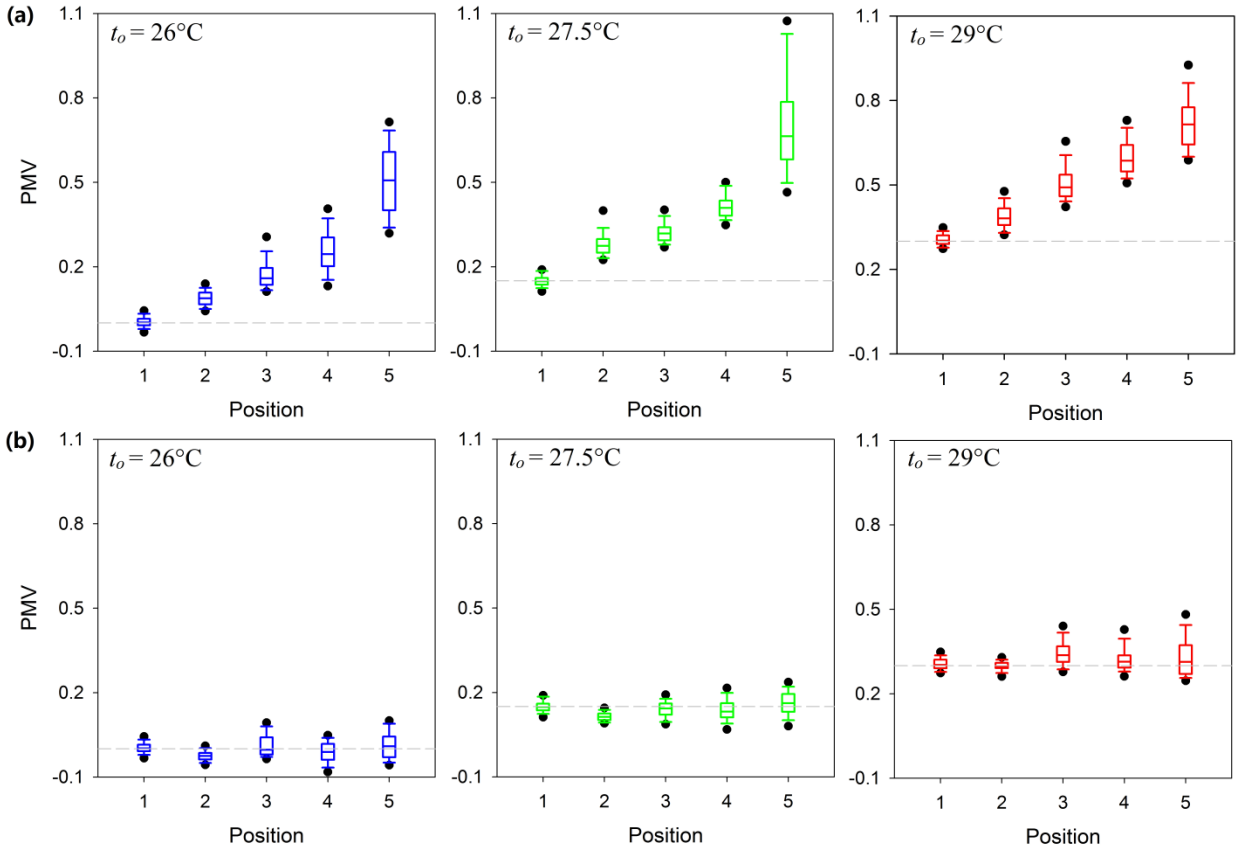

Figure 8: PMV values: (a) without proposed method; (b) with proposed method. The target PMV values, 0.00, 0.15 and 0.30 for 26°C, 27.5°C and 29°C respectively, are shown as dashed lines.

4. Discussion

4.1 Automatic mode and occupant-control mode

The proposed system can actually be set in two different operation modes: the automatic mode and the occupant-control mode. The first mode refers to the methodology described in the paper

and it strictly follows the ASHRAE 55-2013 standard that the air speed should be limited below 0.8 m/s. Thus the fan can be only used up to the 12th scale of speed setting (Table A1 in Supplementary Information). However, this is not applicable for the occupants who want to take control over the thermal conditions. For example, for those who are doing high-metabolic activities or in a situation with high air temperature, air movement can be higher than 0.8 m/s. In this case, the system will give the fan control back to the occupant. In the occupant-control mode, the fan is able to provide as high as 3.0 m/s air speed (Table A1 in Supplementary Information). Therefore the potential of the fan can be fully exploited.

4.2 Multiple-occupants case

The experiments targeted individual occupant but the system can be extended to the case where multiple occupants are detected. If more than one occupant is detected in the same sub-area, the system operates as normal since the fan is able to deliver air flow to the occupants in the same geofenced sub-area simultaneously. If over one occupant is detected in different sub-area, the centroid of the different estimated positions can be calculated. The estimated centroid position can then be used for selecting the suitable calibrated mapping curve to determine the fan power and the fan will swing among them.

4.3 Limitations

The fan used in the proposed system may have a risk of interaction with the lighting system in the environment and the noise generated in high-air-speed condition may cause discomfort. The position of the camera used in the system is fixed to guarantee that the tracking area is covered. This could be improved by installing the camera in the fan in the future.

The use of the camera in the system may have the potential for information leakage. Therefore the system tracks the reference marker placed behind the chair instead of the occupant. This simplified condition can be made more realistic by using existing available algorithm for face or other body parts recognition if privacy is not an issue. It is also possible to improve the system in a way that the information is encrypted and processed implicitly in the camera itself avoiding the privacy or security concern. The images analyzed in the experiments were taken using a normal phone camera for demonstration. In a real-time application, a low-cost indoor camera should be used.

5. Conclusion

In this paper, a tracking cooling fan using geofence and camera-based indoor localization is proposed for thermal comfort improvement and energy savings. The proposed camera-based indoor tracking system is able to accurately locate the positions of the occupant, determine the direction of air flow, and calculate the occupant-fan distance. A calibrated mapping algorithm is also proposed to automatically adjust the fan input power to generate desired air speed determined by the PMV-SET model.

The effectiveness of the proposed system has been verified through experiments. The system can be used in an air-conditioned environment with a higher temperature setpoint to save energy or in a naturally conditioned environment for thermal comfort enhancement.

Acknowledgement

This research is funded by the Republic of Singapore's National Research Foundation through a grant to the Berkeley Education Alliance for Research in Singapore (BEARS) for the Singapore-Berkeley Building Efficiency and Sustainability in the Tropics (SinBerBEST) Program. BEARS has been established by the University of California, Berkeley as a center for intellectual excellence in research and education in Singapore.

Reference

ANSI/ASHRAE (2013). ANSI/ASHRAE standard 55-2013, thermal environmental conditions for human occupancy. *Atlanta, USA: American Society of Heating, Refrigerating and Air-Conditioning Engineers*.

Arens E. A., Turner S., Zhang H., & Paliaga G. (2009). Moving air for comfort. *ASHRAE Journal*, *51(5)*: 18–29.

Arens E. A., Zhang H., & Anwar G. (2015). Interactive occupant-tracking fan for indoor comfort and energy conservation. *U.S. Patent WO2015095753*.

Benezeth, Y., Laurent, H., Emile, B., & Rosenberger, C. (2011). Towards a sensor for detecting human presence and characterizing activity. *Energy and Buildings*, *43*(2), 305-314. doi: 10.1016/j.enbuild.2010.09.014.

Daikin. Daikin room air conditioner operation manual. [Online] http://www.daikinac.com/content/assets/DOC/OperationManuals/FTXS15_18_24LVJU%20Operation%20Manual.pdf (Access date: 28 October 2016).

Dodier, R. H., Henze, G. P., Tiller, D. K., & Guo, X. (2006). Building occupancy detection through sensor belief networks. *Energy and Buildings*, *38*(9), 1033-1043. doi: 10.1016/j.enbuild.2005.12.001.

DOE (2011). Report on the first quadrennial technology review. *United States Department of Energy, Washington, DC*.

Duarte, C., Raftery, P., & Schiavon, S. (2016). SinBerBEST technology energy assessment report. *Building Efficiency and Sustainability in the Tropics*.

Duarte, C., Van Den Wymelenberg, K., & Rieger, C. (2013). Revealing occupancy patterns in an office building through the use of occupancy sensor data. *Energy and Buildings*, *67*, 587-595. doi:10.1016/j.enbuild.2013.08.062.

Gaspar, T., & Oliveira, P. (2015). New depth from focus filters in active monocular vision systems for indoor 3-D tracking. *IEEE Transactions on Control Systems Technology*, *23*(5), 1827-1839. doi: 10.1109/TCST.2015.2388956.

Hoyt, T., Arens, E., & Zhang, H. (2015). Extending air temperature setpoints: Simulated energy savings and design considerations for new and retrofit buildings. *Building and Environment*, *88*, 89-96. doi: 10.1016/j.buildenv.2014.09.010.

Jia, L., & Radke, R. J. (2014). Using time-of-flight measurements for privacy-preserving tracking in a smart room. *IEEE Transactions on Industrial Informatics*, *10*(1), 689-696. doi: 10.1109/TII.2013.2251892.

Kim, H. H., Lee, K. C., & Lee, S. (2013). Location-based human-adaptive air conditioning by measuring physical activity with a non-terminal-based indoor positioning system. *Building and Environment*, *62*, 167-173. doi: 10.1016/j.buildenv.2013.01.020.

Li, N., Calis, G., & Becerik-Gerber, B. (2012). Measuring and monitoring occupancy with a RFID based system for demand-driven HVAC operations. *Automation in Construction*, *24*, 89-99. doi: 10.1016/j.autcon.2012.02.013.

Liu, L. (2013). Multi-mode intelligent sensing tracking fan. *China Patent CN103047162*.

Mautz R. (2012). Indoor positioning technologies. *Ph.D. Dissertation, Habilitation Thesis ETH Zurich*.

Mitsubishi. Kirigamine Move-Eye Sensor Navi-room Air Conditioners. [Online] http://eco.mitsubishielectric.eu/our_products/homes/kirigamine_move-eye_sensor_navi_room_air_conditioners (Access date: 28 October 2016).

McIntyre, D. A. (1978). Preferred air speeds for comfort in warm conditions. *ASHRAE Trans*, *84*(2), 263-277.

Munson, J. P., & Gupta, V. K. (2002). Location-based notification as a general-purpose service. In *Proceedings of the 2nd International Workshop on Mobile Commerce* (pp. 40-44). ACM. doi: 10.1145/570705.570713.

Namiot, D., & Sneps-Sneppe, M. (2013). Geofence and network proximity. In *Proceedings of the 13th International Conference on NEW2AN and the 6th Conference on ruSMART* (pp. 117-127). Springer Berlin Heidelberg. doi: 10.1007/978-3-642-40316-3_11

NCCS & NRF (2011). Air-con system efficiency primer: a summary. *National Climate Change Secretariat and National Research Foundation, Republic of Singapore*.

NEA (2010). Singapore's second national communication: under the united nations framework convention on climate change. *National Environment Agency, Republic of Singapore*.

Ni, L. M., Liu, Y., Lau, Y. C., & Patil, A. P. (2004). LANDMARC: indoor location sensing using active RFID. *Wireless Networks*, *10*(6), 701-710. doi:10.1023/B:WINE.0000044029.06344.dd.

Rana, R., Kusy, B., Wall, J., & Hu, W. (2015). Novel activity classification and occupancy estimation methods for intelligent HVAC (heating, ventilation and air conditioning) systems. *Energy*, *93*, 245-255. doi: 10.1016/j.energy.2015.09.002.

Reclus, F., & Drouard, K. (2009). Geofencing for fleet & freight management. In *Proceedings of the 9th International Conference on Intelligent Transport Systems Telecommunications (ITST)* (pp. 353-356). IEEE. doi: 10.1109/ITST.2009.5399328.

Rim, D., Schiavon, S., & Nazaroff, W. W. (2015). Energy and cost associated with ventilating office buildings in a tropical climate. *PloS One*, *10*(3), e0122310. doi:10.1371/journal.pone.0122310.

Schiavon, S., & Melikov, A. K. (2008). Energy saving and improved comfort by increased air movement. *Energy and Buildings*, *40*(10), 1954-1960. doi: 10.1016/j.enbuild.2008.05.001.

Schiavon, S., Hoyt, T., & Piccioli, A. (2014). Web application for thermal comfort visualization and calculation according to ASHRAE Standard 55. *Building Simulation* (Vol. 7, No. 4, pp. 321-334). Tsinghua University Press. doi: 10.1007/s12273-013-0162-3.

Schiavon S., Yang B., Donner Y., Chang W. C., & Nazaroff W. (2016). Thermal comfort, perceived air quality and cognitive performance when personally controlled air movement is used by tropically acclimatized persons. *Indoor Air*. doi:10.1111/ina.12352.

Sekhar, S. C. (1995). Higher space temperatures and better thermal comfort—a tropical analysis. *Energy and Buildings*, *23*(1), 63-70. doi: 10.1016/0378-7788(95)00932-N.

Sekhar, S. C. (2016). Thermal comfort in air-conditioned buildings in hot and humid climates–why are we not getting it right?. *Indoor air*, *26*(1), 138-152. doi:10.1111/ina.12184.

Shan, K., Sun, Y., Wang, S., & Yan, C. (2012). Development and In-situ validation of a multi-zone demand-controlled ventilation strategy using a limited number of sensors. *Building and Environment*, *57*, 28-37. doi:10.1016/j.buildenv.2012.03.015.

SSC (2009). Singapore standard SS 553:2009: code of practice for air-conditioning and mechanical ventilation in buildings. *Building and Construction Standards Committee, Singapore Standard Council.*

Sun, Z., Wang, S., & Ma, Z. (2011). In-situ implementation and validation of a CO 2-based adaptive demand-controlled ventilation strategy in a multi-zone office building. *Building and Environment*, *46*(1), 124-133. doi:10.1016/j.buildenv:2010.07.008.

Xia, J. J., Yang K. J., Zheng S., Qian, F. L., & Chen H. (2010). Intelligent vertical oscillating fan with automatic tracking capability. *China Patent CN101696697*.

Yang, B., Schiavon, S., Sekhar, C., Cheong, D., Tham, K. W., & Nazaroff, W. W. (2015). Cooling efficiency of a brushless direct current stand fan. *Building and Environment*, *85*, 196-204. doi: 10.1016/j.buildenv.2014.11.032.

Zhai, Y., Zhang, H., Zhang, Y., Pasut, W., Arens, E., & Meng, Q. (2013). Comfort under personally controlled air movement in warm and humid environments. *Building and Environment*, *65*, 109-117. doi: 10.1016/j.buildenv.2013.03.022.

Zhang, Y., & Zhao, R. (2007). Effect of local exposure on human responses. *Building and Environment*, *42*(7), 2737-2745. doi: 10.1016/j.buildenv.2006.07.014.

Zhang, H., Arens, E., Huizenga, C., & Han T. (2010a). Thermal sensation and comfort models for non-uniform and transient environments: part I: local sensation of individual body parts. *Building and Environment* 45, no. 2, 380–388. doi: 10.1016/j.buildenv.2009.06.018.

Zhang, H., Arens, E., Huizenga, C., & Han T. (2010b). Thermal sensation and comfort models for non-uniform and transient environments, part II: local comfort of individual body parts. *Building and Environment* 45, no. 2, 389–398. doi: 10.1016/j.buildenv.2009.06.015.

Zhang, H., Arens, E., Huizenga, C., & Han T. (2010c). Thermal sensation and comfort models for non-uniform and transient environments, part III: whole-body sensation and comfort. *Building and Environment* 45, no. 2, 399–410. doi: 10.1016/j.buildenv.2009.06.020.

Zhou, J., & Shi, J. (2011). A comprehensive multi-factor analysis on RFID localization capability. *Advanced Engineering Informatics*, *25*(1), 32-40. doi:10.1016/j.aei.2010.05.006.

Zhou, X. D., Linghu, J. B., Xu, J. W., Tan L., Qi, K. L., & Fu, X. X. (2014). Control method and device allowing electric fan to track human bodies. *China Patent CN103925225*.

Supplementary information

The fan speed settings, the corresponding fan power and air speeds at tested distances are summarized in Table A1. The fan power was measured using a commercial power meter (Energy monitoring socket, Efergy, UK) with the accuracy of ±2% of readings.

Table A1: Fan speed settings, the corresponding fan power and air speeds at tested distances.

Fan speed settings	Fan power (W)	Average air speed (m/s)								
		0.5 m	1.0 m	1.5 m	2.0 m	2.5 m	3.0 m	3.5 m	4.0 m	4.5 m
1	3.8	0.96	0.77	0.67	0.58	0.46	0.39	0.32	0.31	0.28
2	4.4	1.13	0.93	0.81	0.69	0.54	0.46	0.38	0.37	0.28
3	4.7	1.30	1.07	0.94	0.79	0.65	0.57	0.46	0.44	0.35
4	5.2	1.51	1.20	1.03	0.85	0.72	0.66	0.54	0.51	0.40
5	5.7	1.67	1.29	1.12	0.92	0.79	0.72	0.57	0.55	0.42
6	6.4	1.79	1.38	1.18	0.96	0.84	0.76	0.59	0.58	0.44
7	6.8	1.87	1.44	1.24	1.01	0.85	0.76	0.60	0.59	0.47
8	7.9	2.06	1.53	1.32	1.06	0.94	0.84	0.68	0.64	0.54
9	8.6	2.21	1.64	1.42	1.17	0.98	0.90	0.73	0.69	0.57
10	9.1	2.21	1.66	1.45	1.21	1.00	0.91	0.75	0.71	0.62
11	9.6	2.33	1.73	1.50	1.24	1.02	0.92	0.75	0.69	0.58
12	10.9	2.44	1.81	1.59	1.31	1.04	0.95	0.80	0.73	0.67
13	11.8	2.56	1.87	1.63	1.35	1.13	1.03	0.84	0.78	0.68
14	13.0	2.57	1.85	1.63	1.38	1.14	1.02	0.83	0.77	0.69
15	14.2	2.82	2.00	1.76	1.45	1.16	1.04	0.89	0.80	0.73
16	15.4	2.90	2.05	1.80	1.48	1.28	1.13	0.95	0.85	0.71
17	16.4	3.02	2.11	1.88	1.59	1.33	1.19	1.02	0.92	0.74
18	17.6	2.98	2.11	1.89	1.58	1.30	1.16	1.00	0.90	0.71
19	18.4	2.98	2.05	1.85	1.58	1.32	1.17	0.99	0.85	0.72
20	19.3	3.04	2.15	1.93	1.63	1.37	1.22	1.06	0.93	0.77

The distribution of air speed measurements in Figure 7 is tested for normality using the Shapiro-Wilk normality test. The measurements do not exhibit a normal distribution ($W = 0.98$, $p < 0.05$). The medians (1^{st} quartiles, 3^{rd} quartiles) of all the measured data in Figure 7 and their corresponding PMV values in Figure 8 are summarized in Table A2 and A3, respectively. In Table A2, without the calibrated mapping algorithm, the deviation of the air speed from the target value for each temperature category becomes larger when the occupant-fan distance grows and the objective of achieving the desired air speed cannot be fulfilled. Therefore, the PMV values deviate farther from the targets with increased distance and even go outside the thermal comfort range at farther positions as shown in Table A3.

Table A2: Medians (1^{st} quartiles, 3^{rd} quartiles) of measured air speeds in Figure 7.

Test positions	Mapping algorithm	26°C category: target air speed - 0.55 m/s		27.5°C category: target air speed - 0.64 m/s		29°C category: target air speed - 0.78 m/s	
		Fan power (W)	Measured air speed (m/s)	Fan power (W)	Measured air speed (m/s)	Fan power (W)	Measured air speed (m/s)
1	Used (baseline data)	2.8	0.55(0.53,0.56)	3.2	0.64(0.63,0.66)	3.8	0.78(0.75,0.80)
2	Used	3.3	0.58(0.57,0.60)	3.8	0.69(0.68,0.71)	4.8	0.79(0.77,0.80)
	Not used	2.8	0.45(0.43,0.47)	3.2	0.50(0.48,0.52)	3.8	0.67(0.63,0.70)
3	Used	4.0	0.55(0.50,0.58)	4.7	0.65(0.63,0.68)	6.2	0.73(0.69,0.76)
	Not used	2.8	0.39(0.36,0.40)	3.2	0.46(0.44,0.48)	3.8	0.55(0.51,0.58)
4	Used	4.5	0.56(0.53,0.60)	5.4	0.67(0.63,0.70)	7.3	0.76(0.73,0.80)
	Not used	2.8	0.32(0.29,0.35)	3.2	0.39(0.37,0.41)	3.8	0.47(0.43,0.50)
5	Used	6.0	0.54(0.50,0.59)	7.4	0.63(0.58,0.67)	10.3	0.76(0.68,0.83)
	Not used	2.8	0.20(0.17,0.24)	3.2	0.25(0.21,0.29)	3.8	0.38(0.34,0.42)

Table A3: Medians (1^{st} quartiles, 3^{rd} quartiles) of PMV values in Figure 8.

Test positions	Mapping Algorithm	26°C category: target PMV - 0.00		27.5°C category: target PMV - 0.15		29°C category: target PMV - 0.30	
		Fan power (W)	PMV	Fan power (W)	PMV	Fan power (W)	PMV
1	Used (baseline data)	2.8	0.00(-0.01,0.02)	3.2	0.15(0.14,0.16)	3.8	0.30(0.29,0.32)
2	Used	3.3	-0.03(-0.04,-0.01)	3.8	0.11(0.10,0.13)	4.8	0.30(0.29,0.31)
	Not used	2.8	0.09(0.07,0.11)	3.2	0.27(0.25,0.30)	3.8	0.38(0.36,0.42)
3	Used	4.0	0.00(-0.02,0.04)	4.7	0.14(0.12,0.16)	6.2	0.34(0.31,0.37)
	Not used	2.8	0.16(0.14,0.20)	3.2	0.32(0.29,0.34)	3.8	0.49(0.46,0.54)
4	Used	4.5	-0.01(-0.04,0.02)	5.4	0.13(0.11,0.16)	7.3	0.31(0.29,0.34)
	Not used	2.8	0.25(0.20,0.30)	3.2	0.41(0.38,0.44)	3.8	0.57(0.55,0.64)
5	Used	6.0	0.01(-0.03,0.04)	7.4	0.16(0.13,0.19)	10.3	0.31(0.27,0.37)
	Not used	2.8	0.51(0.40,0.61)	3.2	0.66(0.58,0.79)	3.8	0.71(0.64,0.78)